PCCP

Cite this: *Phys. Chem. Chem. Phys.*, 2011, **13**, 14026–14032

www.rsc.org/pccp

PAPER

The boron–boron single bond in diborane(4) as a non-classical electron donor for hydrogen bonding†‡

Ibon Alkorta,*[a] Ignacio Soteras,[a] José Elguero[a] and Janet E. Del Bene[b]

Received 1st March 2011, Accepted 2nd June 2011
DOI: 10.1039/c1cp20560a

An *ab initio* study of an isomer of diborane(4) [B_2H_4] has been carried out at MP2/aug-cc-pVTZ to investigate the ground-state properties of this unusual molecule, a derivative of which has been described in the recent literature. The geometric, electronic and orbital characteristics of B_2H_4(4) have been analyzed using AIM, NBO, and ELF methodologies. A region with a high concentration of electron density is located near and along the B–B bond, on the opposite side of this bond relative to the bridging H atoms. This site serves as an electron-donor site to electrophiles, resulting in hydrogen-bonded complexes of B_2H_4 with proton donors HF, HNC, HCl, HCN, and HCCH, and a van der Waals complex with H_2. These complexes have C_{2v} symmetry and stabilization energies that vary from 2 to 27 kJ mol^{-1}. The SAPT2 energy decomposition analysis shows that the relative importance of the various terms that contribute to the interaction energy depends on the strength of the interaction.

1. Introduction

Like carbon, silicon, and sulfur, boron is one of the more versatile elements of the Periodic Table since it can also form different types of bonds with itself and with other elements. Thus, B–B single,[1–6] one-electron σ,[7] double,[8–12] aromatic,[13] and triple[14–19] bonds have been reported. In a recent article, a derivative **1** of diborane B_2H_4(4) has been described,[20] in which there are two bridging hydrogen atoms, with each boron atom also bonded to a bulky aromatic substituent. No evidence of other stabilizing interactions was found.

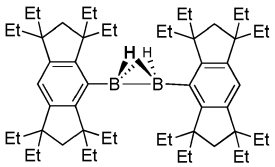

1

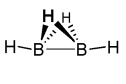

2

3

Previous theoretical investigations have shown that two alternative structures of diborane(4), **2** and **3**, have very similar energies.[3,5] Some metal complexes with an open rather than a bridged structure which resemble structure **3** have been detected experimentally.[21–23] However, an experimental photoionization mass spectrometric investigation concluded that isolated B_2H_4 has structure **2**.[4] This finding led us to investigate the structure and bonding properties of **2**, which is identified as diborane(4). In this paper we characterize this molecule and its hydrogen-bonded complexes with a set of electrophiles.

2. Methods

The geometries of B_2H_4(4), the Lewis acids HF, HCN, HCl, HNC, HCCH, and H_2, and the complexes formed between B_2H_4(4) and these acids were fully optimized at MP2/6-31+G(d,p).[24,25] Frequency calculations were performed at this level to confirm that these structures correspond to minima on their potential surfaces. These monomers and complexes were then re-optimized at MP2/aug-cc-pVTZ.[26] Binding energies have been calculated at this level as the negative of the interaction energy, which is computed as the total energy of the complex minus the sum of the energies of the isolated monomers. This energy has also been computed including the basis set superposition error (BSSE) using the full counterpoise method proposed by Boys and Bernardi.[27] The BSSE corrected MP2/aug-cc-pVTZ interaction energies are closer to the MP2/CBS energies than the uncorrected ones.[28] All of these calculations have been carried out using the Gaussian-09 package.[29]

To gain insight into the nature of the interactions in these complexes, we have carried out several different analyses, including an energy decomposition using symmetry-adapted perturbation theory (SAPT) with the aug-cc-pVTZ basis set. These calculations were performed at the optimized MP2/aug-cc-pVTZ geometries using the SAPT2008 program.[30]

[a] *Instituto de Química Médica, CSIC, Juan de la Cierva, 3, E-28006 Madrid, Spain. E-mail: ibon@iqm.csic.es*
[b] *Department of Chemistry, Youngstown State University, Youngstown, Ohio 44555, USA*

† Thematic issue: Weak Hydrogen Bonds—Strong Effects.

‡ Electronic supplementary information (ESI) available: Figure of the less stable B_2H_4:FH complex and Cartesian coordinates of the complexes calculated at the MP2/aug-cc-pVTZ computational level. See DOI: 10.1039/c1cp20560a

The electron densities of B_2H_4 and its complexes have been analyzed employing the Atoms In Molecules (AIM) methodology[31,32] with the AIMAll program.[33] A value of 0.001 e bohr^{-3} has been used to define the van der Waals surfaces of molecules and to calculate the degree of electron density penetration due to complex formation. Atomic charges have been evaluated by numerical integration of the electron density in the atomic basins. A value of 1×10^{-3} for the integrated magnitude of the Laplacian has been used as a cut-off, since smaller values of this parameter have been shown to provide small average errors in the total charge of the system.[34] The TOPMOD program[35] has been used to analyze the areas of charge concentration in terms of the Electron Localization Function (ELF).[36] ELF is a function that becomes large in regions of space where electron pairs are localized, either as bonding or lone pairs. The function is conveniently scaled between 0 and 1, thereby mapping from the very low (0) to very high (1) electron localization regimes. ELF $>$ 0.5 isosurfaces provide clear pictures of the regions of electron localization in molecules. The ELF basins have been successfully related to key bonding concepts, such as core, valence, and lone-pair regions, while their populations and synaptic orders have been related to bond order. A convenient value of ELF = 0.8 has been adopted in the present work.

Finally, the Natural Bond Orbital (NBO) method[37,38] implemented in Gaussian09 was applied at the B3LYP/aug-cc-pVTZ//MP2/aug-cc-pVTZ level to calculate the atomic charges and analyze energies. The molecular electrostatic potential (MEP) has been calculated to identify regions favorable for electrophilic attack.

3. Results and discussion

3.1 Properties of the isolated molecule

The calculated B–B distance of diborane(4) **2** (1.465 Å) is in reasonably good agreement with the reported value from the X-ray structure of **1** (1.488 Å), despite the difference in the substituents bonded to the boron atoms. The sensitivity of the B–B interatomic distance to substituents can be seen by comparing the B–B distance in the computed structure of the dimethyl derivative of diborane, $CH_3BH_2BCH_3$ **4**, with that of **2**. The dimethyl derivative has a similar structure to **2** but with a B–B distance of 1.474 Å. B_2H_4(4) and its dimethyl derivative are illustrated in Fig. 1.

The electronic properties of isolated **2** have been studied using AIM, ELF and MEP methodologies. The AIM results show the presence of a non-nuclear attractor NNA (a maximum in the electron density) along the B–B bond path, as illustrated in Fig. 2. The presence of a non-nuclear attractor is not

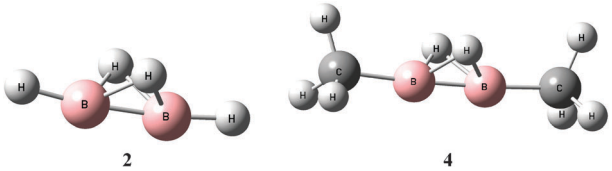

Fig. 1 Optimized MP2/aug-cc-pVTZ structures of B_2H_4(4) and its dimethyl derivative.

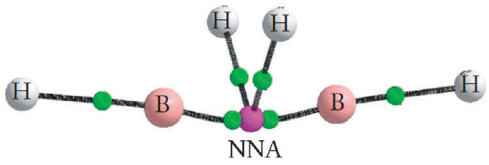

Fig. 2 Molecular graph of B_2H_4 calculated at MP2/aug-cc-pVTZ. The green dots indicate the positions of bond critical points. The NNA is represented in purple. The lines connecting the atoms correspond to the bond paths.

common for systems other than those containing metals. However, several chapters in a recent book discuss NNAs in other situations.[39–41] As the editors note in the opening chapter,[39] local maxima in the electron density can occur occasionally at positions other than those of atomic nuclei, especially in metals and semiconductors. The non-nuclear maxima, or non-nuclear attractors (NNAs), are topologically indistinguishable from nuclear maxima.[42] Thus, similar to a local maximum in the electron density surrounding a nucleus, an NNA is associated with a basin swept by gradient vector field lines and bounded by a zero-flux surface. Consequently, NNA basins constitute proper open quantum systems and have therefore been termed "pseudo-atoms".[43] Pseudo-atoms can be bonded (*i.e.* share a common interatomic zero-flux surface, a bond critical point, or a bond path) to atoms or other pseudo-atoms in a molecule. Non-nuclear attractors and their basins are important for characterizing bonding in such systems.

Particularly relevant to the present investigation is a discussion of boron–boron bonds by Martín Pendás, Blanco, Costales, Mori Sánchez, and Luaña.[44] These authors proposed that rather than being an oddity, NNAs are a normal step in the chemical bonding of homonuclear atoms if the internuclear distance lies within a range conducive to bonding. For boron–boron bonds, the calculated range is between 1.06 and 1.59 Å. Since the B–B distances in **2** and **4** are 1.465 and 1.474 Å, respectively, the appearance of NNAs should not be considered abnormal in these rather unique molecules.

The ELF analysis of B_2H_4(4) indicates the existence of a region of highly localized electron density on the opposite side of the bridging hydrogen atoms of B_2H_4, as shown in Fig. 3. This is the region in which the AIM basin of the NNA is located. The integrated electron density over the ELF basin associated with this region accounts for 2.01 electrons. The Molecular Electrostatic Potential (MEP) of this molecule also shows an important region of negative charge on the opposite side of the B–B bond relative to the bridging hydrogen atoms,

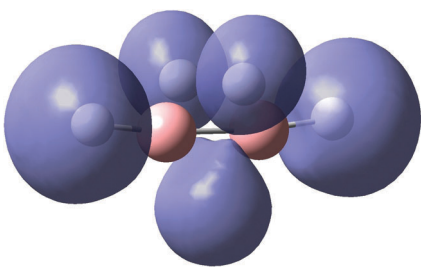

Fig. 3 ELF isosurface at a 0.8 value calculated at the MP2/aug-cc-pVTZ computational level.

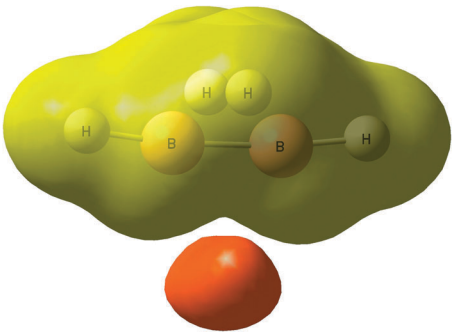

Fig. 4 Molecular electrostatic potential at ±0.03 au calculated at the MP2/aug-cc-pVTZ computational level. Orange and lime green regions indicate negative and positive regions, respectively.

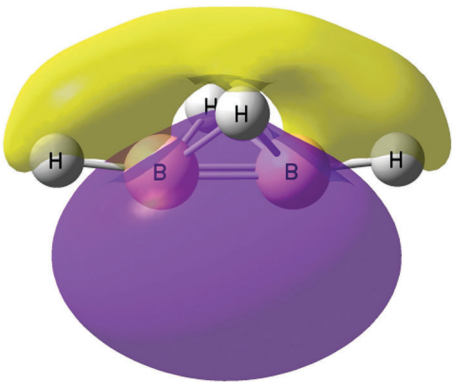

Fig. 5 Representation of the NBO σ_{B-B} molecular orbital at a ±0.02 isosurface.

as shown in Fig. 4. The value of the MEP at the minimum is −0.051 au. All of these indicators suggest that the B–B bond of B_2H_4(4) may serve as an electron donor for the formation of hydrogen bonds.

The NBO analysis provides a straightforward representation of the molecular orbitals of B_2H_4(4). It shows that this molecule has seven doubly-occupied orbitals: two corresponding to the core electrons of the two boron atoms; two corresponding to the axial B–H bonds; two three-center BHB bonds; and one B–B σ bond. The last orbital, the HOMO (Fig. 5), is formed by $sp^{2.2}$ hybrid orbitals on both boron atoms. The individual orbitals point to a region opposite the bridging H atoms significantly below the B–B bond, and thus the bond path linking the two boron atoms with the NNA shows a clear curvature. The region where the B–B σ bond is located corresponds to the region of high electron density previously identified by the ELF and MEP analyses. Thus, it is this region which makes B_2H_4(4) a relatively electron-rich site for hydrogen-bond formation.

3.2 Hydrogen bonded complexes of diborane(4)

3.2.1 Energies and geometries. An initial search of the B_2H_4–FH potential surface led to the identification of minima for two types of hydrogen-bonded complexes. The more weakly-bound complex has FH as the basic site for hydrogen bonding, as illustrated in Fig. S1 of the ESI‡, and a binding energy including BSSE of only 1.6 kJ mol^{-1}. Given this result, searches of potential surfaces for complexes of this type were not carried out. Rather, this investigation has been limited to only those complexes in which B_2H_4(4) acts as the basic site for hydrogen bonding.

Table 1 MP2/aug-cc-pVTZ binding energies (E_i, kJ mol^{-1}), and selected distances (Å)

Complex	E_i	E_i with BSSE	Distance H···*[a]	H···B distance	H–X bond elongation
B_2H_4:HF	29.6	27.1	2.096	2.221	0.039
B_2H_4:HNC	27.3	24.3	2.284	2.399	0.049
B_2H_4:HCl	21.1	18.7	2.271	2.386	0.046
B_2H_4:HCN	15.9	13.8	2.599	2.701	0.025
B_2H_4:HCCH	9.8	8.0	2.733	2.829	0.012
B_2H_4:H_2	1.9	1.6	3.299	3.379	0.002

[a] * indicates the geometrical center of the B–B bond.

MP2/aug-cc-pVTZ binding energies and selected geometric parameters of the complexes of B_2H_4 with Lewis acids HF, HCN, HCl, HNC, HCCH, and H_2 are reported in Table 1. These complexes, illustrated in Fig. 6, have C_{2v} symmetry with the hydrogen atom of the Lewis acid pointing toward the region of the NNA and the negative MEP. The geometries of the B_2H_4:HX complexes resemble the experimental and calculated geometries of the corresponding C_2H_2:HX and C_2H_4:HX complexes.[45–47] When HF is the acid, the distance between the HF proton and the midpoint of the B–B bond is 2.096 Å, which is similar to but shorter than that distance in the corresponding complex C_2H_2:HF (2.19 Å).[45]

The binding energies of these complexes range from 27 kJ mol^{-1} for B_2H_4:HF to less than 2 kJ mol^{-1} for the van der Waals complex formed between B_2H_4 and H_2. These energies are about 1.6 times greater than those computed for the corresponding complexes with C_2H_2.[48] The binding energies of the complexes between C_2H_2 and HF, HCl, HCN and HCCH are reported in ref. 48. For comparison purposes, the complexes of C_2H_2 with HNC and H_2 were reoptimized at MP2/aug-cc-pVTZ.

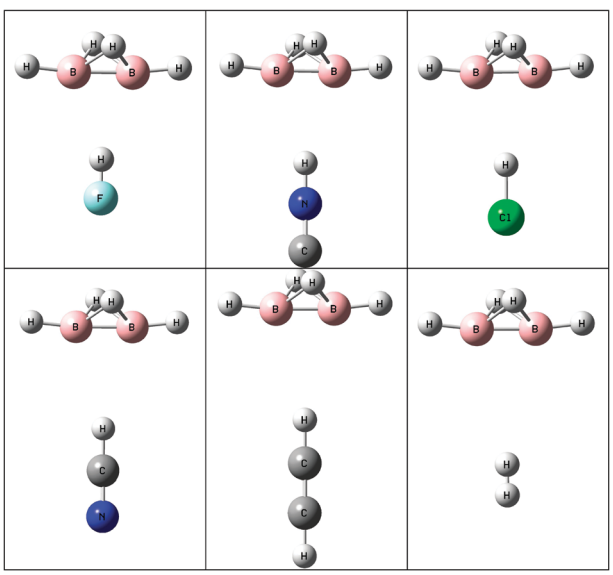

Fig. 6 Hydrogen-bonded complexes of B_2H_4(4) with proton donors and the van der Waals complex with H_2.

Complex formation has little effect on the geometry of B_2H_4, since the B–B distance in isolated B_2H_4 is 1.465 Å, compared to 1.468 Å in the most strongly-bound complex. In contrast, a significant lengthening of the H–X bond of the Lewis acid is observed, in agreement with the trend found for most hydrogen-bonded complexes.[49] Because of the different nature of these H–X bonds, changes in the H–X distances upon complex formation have been normalized using eqn (1) proposed previously by Grabowski.[50]

$$\delta_{XH} = \frac{(r_{X-H} - r^0_{X-H})}{r^0_{X-H}} \quad (1)$$

where r_{X-H} and r^0_{X-H} represent the bond distance in the complex and in the isolated monomer, respectively. δ_{XH} for the diborane(4) complexes investigated in this study is linearly related to the interaction energies of the complexes, with a correlation coefficient (R^2) of 0.94.

3.2.2 Electron density analysis. Table 2 presents values of the electron density, Laplacian, and energy density at bond critical points (ρ_{bcp}, $\nabla^2\rho_{bcp}$, and H_{bcp}, respectively), the amount of charge transfer (CT), electron population of the NNA (σ_{NNA}), and the extent of electron density penetration (σ_S) in the hydrogen-bonded complexes. The intermolecular bond critical points (bcp) are characteristic of hydrogen-bond formation. The bond path links the proton donor with the NNA of the B_2H_4 molecule, as illustrated in Fig. 7. Based on the criteria proposed by Koch and Popelier,[51] the B_2H_4:H_2 complex should not be considered as hydrogen bonded but as a van der Waals complex, since ρ_{bcp} is near the lower limit for hydrogen-bonding interactions (0.002 au). An exponential relationship with a correlation coefficient of 0.999 is found between ρ_{bcp} and the intermolecular distances in these complexes. Similar relationships have been described for a large variety of hydrogen-bonded complexes.[52,53]

Among the complexes with B_2H_4(4), those with HF, HNC, and HCl have the greatest binding energies and positive values of the Laplacian at the bcp. However, the negative values of the total energy density suggest that the hydrogen bonds in these complexes are of intermediate strength.[54] The positive values of both $\nabla^2\rho_{bcp}$ and H_{bcp} for the complexes with HCN and HCCH are indicative of weak hydrogen bonds, and are consistent with the small binding energies of these complexes.

As anticipated, charge transfer occurs from the base B_2H_4(4) to the proton donor. The amount of charge transfer

Table 2 AIM data for electron densities (ρ_{bcp}), Laplacians ($\nabla^2\rho_{bcp}$) and energy densities (H_{bcp}) at bond critical points, charge transfer (CT), variation of the population of the NNA basins (σ_{NNA}), and the extent of electron density penetration (σ_S) in hydrogen-bonded complexes of B_2H_4[a]

	ρ_{bcp}	$\nabla^2\rho_{bcp}$	H_{bcp}	CT	$\Delta\sigma_{NNA}$	σ_S
B_2H_4:HF	0.027	0.035	−0.004	0.067	−0.032	1.253
B_2H_4:HNC	0.019	0.034	−0.001	0.049	−0.030	1.086
B_2H_4:HCl	0.021	0.034	−0.001	0.055	−0.022	1.190
B_2H_4:HCN	0.011	0.025	0.001	0.026	−0.012	0.858
B_2H_4:HCCH	0.008	0.021	0.001	0.018	−0.002	0.747
B_2H_4:H_2	0.003	0.009	0.001	0.007	−0.000	0.259

[a] Values in au, except for σ_S which is in Å.

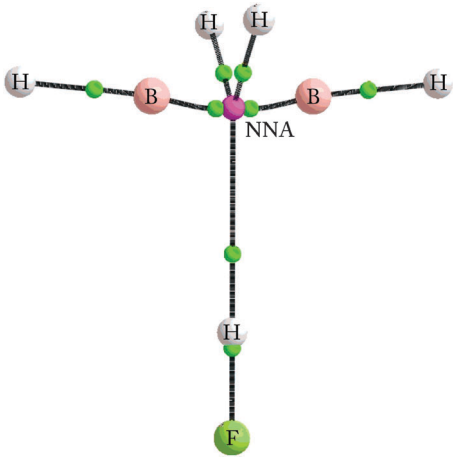

Fig. 7 Molecular graph of the B_2H_4:HF complex calculated at MP2/aug-cc-pVTZ. The green dots indicate the positions of bond critical points. The NNA is given in purple. The lines connecting the atoms correspond to the bond paths.

varies between 0.007 to 0.067 e, with the more strongly bound complexes having the greater amount of charge transfer. Linear correlations exist between the total charge transfer and the interaction energy, and between the total charge transfer and the normalized lengthening of the H–X bond of the Lewis acid (δ_{HX}) with correlation coefficients of 0.91 and 0.98, respectively.

In addition, the population of the NNA shows that approximately half of the charge lost by B_2H_4 comes from this region. The loss of electrons from the NNA basin reduces its volume by 20% in the B_2H_4:HF complex. This loss can arise in part from the electron density penetration of the two interacting molecules, which can be seen from the data of Table 2. As expected, a linear correlation exists between increasing electron density penetration and decreasing intermolecular distance. The changes in the electron density distribution due to complex formation have been mapped for B_2H_4:HF in Fig. 8. The hydrogen atoms and the NNA of B_2H_4 lose electron density, while the intermolecular region and the

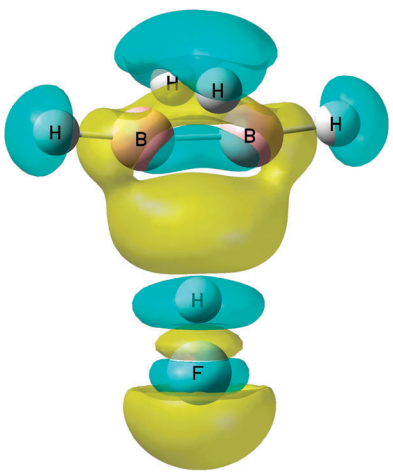

Fig. 8 Electron density shift for the B_2H_4:HF complex at ±0.0005 au isosurfaces. Blue and yellow regions indicate regions of decreased and increased electron density, respectively.

fluorine atom gain electron density. Thus, the total charge lost by B_2H_4 has two sources: the hydrogen atoms and the NNA, as evident from a reduction in its volume.

3.2.3 NBO analysis. The NBO analysis provides insight into charge transfer in intermolecular interactions from an orbital viewpoint. In typical hydrogen-bonded complexes, charge transfer usually involves the highest occupied σ orbital of the electron donor (a lone-pair orbital) and the lowest unoccupied σ* orbital of the electron acceptor. For the complexes with B_2H_4, the highest occupied σ_{B-B} orbital of B_2H_4 is illustrated in Fig. 5, and is the orbital primarily involved in charge transfer to the σ* orbital of the proton donor. The orbital interaction in these complexes can be related to the stabilization energy by means of second-order perturbation theory according to eqn (2). This energy arises from the maximum overlap of the two orbitals involved in charge transfer.

$$E(2)(\sigma_{B-B} \rightarrow \sigma^*_{HX}) = -2\langle\sigma_{B-B}|F|\sigma^*_{XH}\rangle^2/[\varepsilon(\sigma^*_{HX}) - \varepsilon(\sigma_{B-B})] \quad (2)$$

The binding energy and the amount of charge transfer arising from this orbital interaction, and the total amount of molecular charge transfer, are reported in Table 3. In some cases values of $E(2)$ provide estimates of relative binding energies, but only when the interacting molecules belong to a family of compounds,[38] which is not true for the proton-donor molecules included in this study. Moreover, a direct comparison of $E(2)$ and E_i is not valid, since $E(2)$ is a B3LYP energy while E_i is an MP2 energy. Unfortunately, a second order perturbation analysis cannot be carried out at MP2. Nevertheless, it is clear that interaction between the σ_{B-B} orbital and the empty H–X σ* orbital is important in the stabilization of these complexes.

In hydrogen-bonded complexes, charge transfer from the σ_{B-B} orbital to the σ^*_{HX} orbital is a significant portion of the total electron density transferred between the two interacting molecules. For the B_2H_4:HF complex, it accounts for 44% of the total charge transfer. Charge transfer to the H–X σ* orbital is accompanied by an elongation of the H–X bond in the complex relative to the isolated monomer, as evident from Table 1. As expected, the amount of charge transferred and the normalized elongation of the H–X bond (δ_{HX}) are linearly correlated with a correlation coefficient of 0.95. Although the total charge transferred in a particular complex obtained with the NBO method is approximately half of that calculated employing AIM, both methodologies provide a similar qualitative picture of the charge-transfer process.

Table 3 $E(2)$, charge transfer from the $\sigma_{B-B} \rightarrow \sigma^*_{HX}$ orbital, and total charge transfer (CT) calculated within the NBO methodology

Complex	$E(2)$ $\sigma_{B-B} \rightarrow \sigma^*_{HX}$/ kJ mol^{-1}	$\sigma_{B-B} \rightarrow \sigma^*_{HX}$ charge transfer/e	CT/e
B_2H_4:HF	45.6	0.015	0.034
B_2H_4:HNC	34.5	0.011	0.031
B_2H_4:HCl	35.7	0.008	0.040
B_2H_4:HCN	13.1	0.004	0.014
B_2H_4:HCCH	7.2	0.002	0.007
B_2H_4:H_2	1.4	0.000	0.002

3.2.4 SAPT2 analysis. SAPT2 calculations provide a tool for analyzing the interaction energy when two monomers form a complex. In the SAPT2 method, the total interaction energy for a complex is evaluated as the sum of the first- and second-order perturbation terms, without performing a supermolecule calculation. These terms represent well-defined physical contributions to the interaction energy. Since SAPT2 and MP2 are similar but different methodologies, the interaction energies computed using these two methods are different, but they are linearly related, as illustrated in Fig. 9.

Within the SAPT2 framework, the interaction energy (the negative of the binding energy) can be decomposed as shown in eqn (3). The first four terms represent the electrostatic (U_{ele}), induction (U_{ind}), exchange (U_{exc}) and dispersion (U_{dis}) components. In addition, the SAPT2 expansion yields two terms corresponding to the coupling between exchange and induction ($U_{exc-ind}$), and between exchange and dispersion ($U_{exc-dis}$). Finally, the last term (δ_{HF}) accounts for a collection of higher order induction and exchange–induction terms.

$$U^{SAPT2}_{tot} = U_{ele} + U_{ind} + U_{exc} + U_{dis} + U_{exc-ind} + U_{exc-dis} + \delta_{HF} \quad (3)$$

For ease of analysis, the coupling term between exchange and dispersion, $U_{exc-dis}$, which is usually less than 4 kJ mol^{-1}, has been added to the dispersion component, U_{dis}. Similarly, the exchange–induction and higher-order induction terms

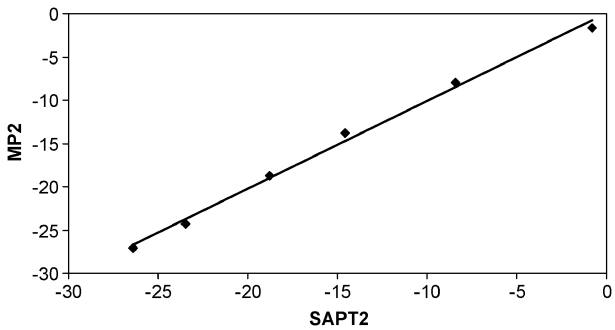

Fig. 9 MP2 *vs.* SAPT2 interaction energies (kJ mol^{-1}). The fitted linear relationship is MP2 = 1.01 SAPT2, R^2 = 0.995.

Table 4 Component of the SAPT2 energy analysis (kJ mol^{-1})

Component	B_2H_4:HF	B_2H_4:HNC	B_2H_4:HCl	B_2H_4:HCN	B_2H_4:HCCH	B_2H_4:H_2
Electrostatic	−44.4	−35.6	−32.6	−19.7	−11.7	−1.7
Exchange	54.8	41.4	49.0	20.5	14.2	3.3
Induction	−23.8	−16.7	−18.4	−7.5	−3.8	−0.4
Dispersion	−13.0	−12.6	−16.7	−7.9	−7.1	−2.1
Total	−26.4	−23.5	−18.8	−14.6	−8.4	−0.8

associated with the $U_{exc-ind}$ and δ_{HF} components have been added to the pure induction component, U_{ind}.

As evident from Table 4, the largest contribution to the interaction energy is the exchange component, which destabilizes the complex. The most important stabilizing component is the electrostatic interaction, except for the van der Waals complex B_2H_4:H_2 for which the dispersion term is slightly more negative than the electrostatic one. For the three complexes (B_2H_4:HF, B_2H_4:HNC and B_2H_4:HCl) with the greatest interaction energies, the second most important attractive component corresponds to the induction term, which is equal to approximately half of the electrostatic term. The dispersion component makes the smallest contribution.

As the interaction energy of a complex decreases, the dispersion term becomes more important than the induction term. Thus, the dispersion term is only slightly more stabilizing than the induction term in the B_2H_4:HCN complex. In the B_2H_4:HCCH complex the dispersion interaction is about twice as large as the induction, while in B_2H_4:H_2 it is five times greater. It is important to note that the relative importance of the various components of the interaction energy as obtained for the complexes with B_2H_4(4) is similar to their importance in other hydrogen-bonded complexes. For hydrogen-bonded complexes the electrostatic and exchange terms are also the two dominant contributors to the interaction energy. For example, a SAPT2 analysis of the interaction energy of the HF dimer (-17.6 kJ mol^{-1}) indicates that the electrostatic interaction is the dominant contributor (-27.2 kJ mol^{-1}) followed by the exchange term (25.9 kJ mol^{-1}). The smallest contributors in hydrogen-bonded complexes are the induction and dispersion terms, with induction more important for strongly-bound complexes, and dispersion more important for weakly-bound complexes.[55]

4. Conclusions

An *ab initio* study of diborane(4) [B_2H_4] has been carried out at MP2/aug-cc-pVTZ. AIM, ELF, and NBO analyses indicate the existence of a region of highly localized electron density located near and along the B–B bond on the opposite side of the bridging hydrogen atoms, which provides an interaction site for electrophiles. Thus, B_2H_4(4) acts as an electron donor and forms hydrogen-bonded complexes of C_{2v} symmetry with the proton donors HF, HNC, HCl, HCN, and HCCH, and a van der Waals complex with H_2. The complex binding energies range from 2 to 27 kJ mol^{-1}, which indicates that these complexes are more stable than the corresponding complexes with C_2H_2. The interaction energies have also been subjected to a SAPT2 analysis. For all hydrogen-bonded complexes, the exchange energy makes the most important contribution to the interaction energy, followed by the electrostatic contribution. The relative importance of the induction and dispersion terms depends on the strength of the interaction.

Acknowledgements

This work was supported by the Ministerio de Ciencia e Innovación (Project No. CTQ2009-13129-C02-02) and Comunidad Autónoma de Madrid (Project MADRISOLAR2, ref. S2009/PPQ-1533). The authors thank the CTI (CSIC) for allocation of computer time.

References

1 R. Weiss and R. N. Grimes, *J. Am. Chem. Soc.*, 1978, **100**, 1401–1405.
2 M. A. Vincent and H. F. Schaeffer III, *J. Am. Chem. Soc.*, 1981, **103**, 5677–5680.
3 R. R. Mohr and W. N. Lipscomb, *Inorg. Chem.*, 1986, **25**, 1053–1057.
4 B. Ruscik, M. Schwarz and J. Berkowitz, *J. Chem. Phys.*, 1989, **91**, 4576–4581.
5 J. F. Stanton, J. Gauss, R. J. Bartlett, T. Helgaker, P. Jørgensen, H. J. A. Jensen and P. R. Taylor, *J. Chem. Phys.*, 1992, **97**, 1211–1216.
6 A. Szabo, A. Kovács and G. Frenking, *Z. Anorg. Allg. Chem.*, 2005, **631**, 1803–1809.
7 J. D. Hoefelmeyer and F. P. Gabbaï, *J. Am. Chem. Soc.*, 2000, **122**, 9054–9055.
8 A. Moezzi, M. M. Olmstead and P. P. Power, *J. Am. Chem. Soc.*, 1992, **114**, 2715–2717.
9 Y. Wang, B. Quillian, P. Wei, C. S. Wannere, Y. Xie, P. B. King, H. F. Schaeffer III, P. v. R. Schleyer and G. H. Robinson, *J. Am. Chem. Soc.*, 2007, **129**, 12412–12413.
10 F.-D. Ren, D.-L. Cao, W.-L. Wang, J. Ren and S.-S. Chen, *THEOCHEM*, 2009, **896**, 38–43.
11 P. P. Power, *Inorg. Chim. Acta*, 1992, **198–200**, 443–447.
12 I. Alkorta, J. E. Del Bene, J. Elguero, O. Mó and M. Yáñez, *Theor. Chem. Acc.*, 2009, **124**, 187–195.
13 H.-S. Wu, H. Jiao, Z.-X. Wang and P. v. R. Schleyer, *J. Am. Chem. Soc.*, 2003, **125**, 4428–4429.
14 M. Zhou, N. Tsumori, Z. Li, K. Fan, L. Andrews and Q. Xu, *J. Am. Chem. Soc.*, 2002, **124**, 12936–12937.
15 M. Zhou, Z.-X. Wang, P. v. R. Schleyer and Q. Xu, *ChemPhysChem*, 2003, **4**, 763–766.
16 F.-D. Ren, D.-L. Cao, W.-L. Wang, J.-L. Wang, Y.-X. Li, Z.-Y. Hu and S.-S. Chen, *Chem. Phys. Lett.*, 2008, **455**, 32–37.
17 S.-D. Li, H.-J. Zhai and L.-S. Wang, *J. Am. Chem. Soc.*, 2008, **130**, 2573–2579.
18 D.-L. Cao, F.-D. Ren, S.-N. Liu and S.-S. Chen, *THEOCHEM*, 2009, **913**, 221–227.
19 X.-F. Dong, F.-D. Ren, D.-L. Cao, W.-N. Wang and F.-Q. Zhang, *THEOCHEM*, 2010, **961**, 73–82.
20 Y. Shoji, T. Matsuo, D. Hashizume, H. Fueno, K. Tanaka and K. Tamao, *J. Am. Chem. Soc.*, 2010, **132**, 8258–8260.
21 S. A. Snow, M. Shimoi, C. D. Ostler, B. K. Thompson, G. Kadama and R. W. Parry, *Inorg. Chem.*, 1984, **23**, 511.
22 K. Katoh, M. Shimoi and H. Ogino, *Inorg. Chem.*, 1992, **31**, 670.
23 R. W. Parry and G. Kodama, *Coord. Chem. Rev.*, 1993, **128**, 245–260.
24 C. Møller and M. S. Plesset, *Phys. Rev.*, 1934, **46**, 618–622.
25 P. A. Hariharan and J. A. Pople, *Theor. Chim. Acta*, 1973, **28**, 213–222.
26 T. H. Dunning, Jr, *J. Chem. Phys.*, 1989, **90**, 1007–1023; D. E. Woon and T. H. Jr Dunning, *J. Chem. Phys.*, 1995, **103**, 4572–4585.
27 S. F. Boys and F. Bernardi, *Mol. Phys.*, 1970, **19**, 553–566.
28 I. Alkorta, C. Trujillo, J. Elguero and M. Solimannejad, *Comput. Theor. Chem.*, 2011, **967**, 147–151.
29 M. J. Frisch, G. W. Trucks, H. B. Schlegel, G. E. Scuseria, M. A. Robb, J. R. Cheeseman, G. Scalmani, V. Barone, B. Mennucci, G. A. Petersson, H. Nakatsuji, M. Caricato, X. Li, H. P. Hratchian, A. F. Izmaylov, J. Bloino, G. Zheng, J. L. Sonnenberg, M. Hada, M. Ehara, K. Toyota, R. Fukuda, J. Hasegawa, M. Ishida, T. Nakajima, Y. Honda, O. Kitao, H. Nakai, T. Vreven, J. A. Montgomery, Jr., J. E. Peralta, F. Ogliaro, M. Bearpark, J. J. Heyd, E. Brothers, K. N. Kudin, V. N. Staroverov, R. Kobayashi, J. Normand, K. Raghavachari, A. Rendell, J. C. Burant, S. S. Iyengar, J. Tomasi, M. Cossi, N. Rega, J. M. Millam, M. Klene, J. E. Knox, J. B. Cross, V. Bakken, C. Adamo, J. Jaramillo, R. Gomperts, R. E. Stratmann, O. Yazyev, A. J. Austin, R. Cammi, C. Pomelli, J. W. Ochterski, R. L. Martin, K. Morokuma,

V. G. Zakrzewski, G. A. Voth, P. Salvador, J. J. Dannenberg, S. Dapprich, A. D. Daniels, O. Farkas, J. B. Foresman, J. V. Ortiz, J. Cioslowski and D. J. Fox, *Gaussian 09*, Gaussian, Inc., Wallingford CT, 2009.
30 SAPT2008: "An Ab initio Program for Many-Body Symmetry-Adapted Perturbation Theory Calculations of Intermolecular Interaction Energies" by R. Bukowski, W. Cencek, P. Jankowski, B. Jeziorski, M. Jeziorska, S. A. Kucharski, V. F. Lotrich, A. J. Misquitta, R. Moszynski, K. Patkowski, R. Podeszwa, S. Rybak, K. Szalewicz, H. L. Williams, R. J. Wheatley, P. E. S. Wormer, and P. S. Żuchowski.
31 R. F. W. Bader, *Atoms in Molecules: A Quantum Theory, The International Series of Monographs of Chemistry*, ed. J. Halpen and M. L. H. Green, Clarendon Press, Oxford, 1990.
32 P. L. A. Popelier, *Atoms in Molecules: An Introduction*, Prentice Hall, 2000.
33 T. A. Keith, *AIMAll, Version 08.11.29*, 2008; aim.tkgristmill.com.
34 I. Alkorta and O. Picazo, *ARKIVOC*, 2005, **ix**, 305–320.
35 S. Noury, X. Krokidis, F. Fuster and B. Silvi, *ToPMoD*, Universite Pierre et Marie Curie, Paris, 1999.
36 B. Silvi and A. Savin, *Nature*, 1994, **371**, 683–686.
37 A. E. Reed, L. A. Curtiss and F. Weinhold, *Chem. Rev*., 1988, **88**, 899–926.
38 F. Weinhold and C. Landis, *Valency and Bonding, A Natural Bond Orbital Donor–Acceptor Perspective*, Cambridge University Press, 2005.
39 C. F. Matta and R. J. Boyd, *An Introduction to the Quantum Theory of Atoms in Molecules*, in *The Quantum Theory of Atoms in Molecules*, ed. Chérif F. Matta and Russell J. Boyd, Wiley-VCH Verlag GmbH & Co. KGaA, Weinheim, 2007, ch. 1.
40 C. Gatti, *Solid State Applications of QTAIM and the Source Function – Molecular Crystals, Surfaces, Host–Guest Systems and Molecular Complexes*, in *The Quantum Theory of Atoms in Molecules*, ed. Chérif F. Matta and Russell J. Boyd, Wiley-VCH Verlag GmbH & Co. KGaA, Weinheim, 2007, ch. 7.
41 V. Luaña, M. A. Blanco, A. Costales, P. Mori-Sánchez and A. M. Pendás, in *The Quantum Theory of Atoms in Molecules*, ed. Chérif F. Matta and Russell J. Boyd, Wiley-VCH Verlag GmbH & Co. KGaA, Weinheim, 2007.
42 C. Gatti, R. Fantucci and G. Pacchioni, *Theor. Chim. Acta*, 1987, **72**, 433–458.
43 W. L. Cao, C. Gatti, P. J. MacDougall and R. F. W. Bader, *Chem. Phys. Lett*., 1987, **141**, 380–385.
44 A. M. Pendás, M. A. Blanco, A. Costales, P. M. Sánchez and V. Luaña, *Phys. Rev. Lett*., 1999, **83**, 1930–1933.
45 I. Rozas, I. Alkorta and J. Elguero, *J. Phys. Chem. A*, 1977, **101**, 9457–9463.
46 A. C. Legon, P. D. Aldrich and W. H. Flygare, *J. Chem. Phys*., 1981, **75**, 625–630.
47 P. D. Aldrich, S. G. Kukolich and E. J. Campbell, *J. Chem. Phys*., 1983, **78**, 3251–3260.
48 S. Scheiner and S. Grabowski, *THEOCHEM*, 2002, **615**, 209–218.
49 S. Scheiner, *Hydrogen Bonding*, Oxford University Press, New York, 1997.
50 S. J. Grabowski, *Chem. Phys. Lett*., 2001, **338**, 361–366.
51 U. Koch and P. Popelier, *J. Phys. Chem*., 1995, **99**, 9747–9754.
52 I. Mata, I. Alkorta, E. Molins and E. Espinosa, *Chem.-Eur. J*., 2010, **16**, 2442–2452.
53 O. Picazo, I. Alkorta and J. Elguero, *J. Org. Chem*., 2003, **68**, 7485–7489.
54 I. Rozas, I. Alkorta and J. Elguero, *J. Am. Chem. Soc*., 2000, **122**, 11154–11161.
55 J. Wu, J. Zang, Z. Wang and W. Cao, *Chem. Phys*., 2007, **338**, 69–74.

